https://doi.org/10.48048/tis.2023.6826

Improving the Performance of Wood Adhesive with Waste Rubber Tire

Suradet Matchawet[1], Jobish Johns[2], Jutatip Artchomphoo[3], Kwanruethai Boonsong[3] and Uraiwan Sookyung[3,*]

[1]Faculty of Science Technology and Agriculture, Yala Rajabhat University, Yala 95000, Thailand
[2]Department of Physics, Rajarajeswari College of Engineering, Karnataka 560074, India
[3]Department of Science, Faculty of Science and Technology, Rajamangala University of Technology Srivijaya, Nakhon Si Thammarat Campus, Nakhon Si Thammarat 80110, Thailand

([*]Corresponding author's e-mail: uraiwan.so@rmutsv.ac.th)

Received: 5 March 2023, Revised: 28 March 2023, Accepted: 29 March 2023, Published: 26 April 2023

Abstract

Reclaimed rubber (RR) from waste tires was introduced as a wood adhesive by blending with epoxidized natural rubber (ENR). To improve the polarity of RR and compatibility with ENR, maleic anhydride (MA) was grafted onto RR chains. Influences of RR and RR-g-MA (maleic anhydride grafted reclaimed rubber) on the adhesion of wood adhesive along with their properties such as crosslinking, mechanical properties, thermal stability, and wettability were studied. It was found that RR and RR-g-MA affect the vulcanization of ENR by increasing crosslink density. Especially, in the case of using RR-g-MA generates a new form of an ester linkage. The higher crosslink density together with the formation of ester linkages results in superior thermal stability by the addition of RR-g-MA. In addition, the incorporation of RR exhibited an increase in the lap shear strength when compared with the pure ENR. This improvement is due to the increased crosslink density because the presence of RR resulted in the enhanced cohesive strength of rubber adhesive. Additionally, the incorporation of RR-g-MA showed higher efficiency to improve the adhesion of rubber adhesive. The addition of RR-g-MA has not only enhanced the cohesive strength of rubber adhesive, but also increased the adhesive strength from the interaction between the hydroxy group in cellulose on the wood surface and the polar functional group (i.e., oxirane rings of ENR, maleic group of RR-g-MA and ester group of ester linkage) of rubber adhesive. Therefore, the cohesive fracture was observed in ENR/RR-g-MA adhesive.

Keywords: Epoxidized natural rubber, Wood adhesive, Reclaimed rubber, Lap shear strength, Waste Rubber Tire, Maleic anhydride, Ester linkage

Introduction

The growing use of rubber products depends on the development of automotive parts because around 65 % of rubber products are used in the automotive industry. It has been reported that approximately 1000 million worn-out waste tires are disposed every year, and predicting the current trend indicated that it will increase to 1200 million by the year 2030 [1,2]. Therefore, a huge volume of waste tires will be released into the environment and directly affects the ecosystem. A waste tire is vulcanized rubber waste that cannot be easily reprocessed and recycled. Several methods were used for the disposal of a waste tires including incineration [3], landfilling [4,5], and reclaiming [6,7]. However, it has been known that incineration and landfilling can cause many problems for the environment by releasing greenhouse gases in the air, reducing biodiversity, and contaminating the environment by leaching soluble toxic components into the soil/or water, respectively. Hence, rubber reclaiming is effective recycling method applied to the waste rubber tire. It uses mechanical, thermal, thermo-mechanical, chemo-thermomechanical, and irradiation energies to break down vulcanized bonds in vulcanized rubber networks [8]. The main rubber components of tires compose natural rubber (NR), butadiene rubber (BR), and styrene butadiene rubber (SBR) [9].

It is a challenge for the rubber industry to turn the recycling rubber waste into a usable products. Rubber reclaiming and blending with virgin rubber has increased in interest in recent times due to the growing concerns about the environment and rising prices of synthetic rubber. The incorporation of reclaimed rubber in rubber formulations reduces the cost of rubber compounds by lowering the loading level of virgin rubber. Previous researchers have studied the blending of reclaimed rubber with various types of virgin rubbers including NR [10-13], BR [10,14], SBR [15-18], ethylene-propylene-diene rubber (EPDM) [19,20], acrylonitrile butadiene rubber (NBR) [21,22]. It can be seen that most of the studies have been focused on blending reclaimed rubber with nonpolar rubbers as they have a closer polarity, whereas,

blending with polar rubber remains quite inadequate. To increase the range of applications and to add the commercial value to NR, epoxidized natural rubber (ENR) was used in the present work. ENR is a modified NR with an epoxy group onto the structure of NR that makes it polar. The advantages of hydrophilic surfaces of ENR by epoxy group gave the benefits in the adhesion with polar substances such as polar polymer, wood, metal, glass fibers etc. Therefore, in the present work, ENR blend with reclaimed rubber (RR), or maleic anhydride grafted reclaimed rubber (RR-g-MA) was studied to apply as a wood adhesive. Influences of RR and RR-g-MA on the adhesion of wood adhesive along with the properties such as crosslinking, mechanical properties, thermal stability and wettability has been thoroughly studied.

Materials and methods

Materials

Reclaimed rubber (RR) was supplied by N.D. Rubber Public Company Limited, Chonburi, Thailand. Epoxidized natural rubber with 25 mol% epoxides (ENR25) was manufactured by Muang Mai Guthrie Public Company Limited, Phuket, Thailand. Maleic anhydride (MA) was manufactured by Sigma-Aldrich. Zinc oxide (ZnO) was manufactured by Lanxess Deutschland GmbH, Germany. Stearic acid was manufactured by Imperial Chemical Co., Ltd., Pathum Thani, Thailand. Wing Stay L was supplied by Kij Paiboon Chemical Part., Ltd., Bangkok, Thailand. Zinc Diethyldithiocarbamate (ZDEC), Zinc-2-mercaptobenzthiazole (ZMBT), and sulfur was manufactured by Petch Thai Chemical Co., Ltd., Bangkok, Thailand.

Preparation of maleic anhydride grafted reclaimed rubber

Maleic anhydride grafted reclaimed rubber (RR-g-MA) with 4 % by weight of maleic anhydride was prepared by melt mixing method in an internal mixer at 60 °C with a rotor speed of 60 rpm for 10 min. Then, RR-g-MA was sheeted out using two roll mills. The grafting reaction was confirmed by Attenuated Total Reflection-Fourier Transform Infrared Spectroscopy (ATR-FTIR).

Preparation of rubber compound and vulcanizates

Compounding formulations including ENR, ENR/RR blends and ENR/RR-g-MA blends are shown in **Table 1**. Rubber compounds were prepared by mixing method in an internal mixer at 60 °C with a rotor speed of 60 rpm with a fill factor of 0.8. The compounding process was started by masticating epoxidized natural rubber for 2 min and RR or RR-g-MA was added. Further, the continuous mixing proceeded for another 2 min. Then, the other ingredients; wing stay L, zinc oxide, stearic acid, and wood rosin were sequentially added and mixed for 1 min each. Subsequently, rubber compounds were removed from the mixing chamber, sheeted out using two roll mills, and kept at room temperature for at least 24 h before the incorporation of ZDEC, ZMBT, and sulfur in a two roll mills. The rubber compounds were then vulcanized in a compression molding machine at 150 °C using the optimum cure time (TC_{90}) which was previously determined by the Moving Die Rheometer (MDR).

Table 1 Compounding formulations of rubber compounds.

Chemical	Rubber formulations (phr)		
	ENR	ENR/RR	ENR/RR-g-MA
ENR25	100	80	80
RR	-	20	-
RR-g-MA	-	-	20
Wing stay L	0.5	0.5	0.5
Zinc Oxide	5	5	5
Stearic acid	2	2	2
Wood rosin	20	20	20
ZDEC	0.7	0.7	0.7
ZMBT	0.3	0.3	0.3
Sulfur	3	3	3

Testing and characterizations

ATR-FTIR

ATR-FTIR (Alpha, Bruker Hong Kong Limited) was used to confirm the grafting reaction between reclaimed rubber and maleic anhydride. RR-g-MA was purified by extracting the unreacted maleic anhydride by re-precipitation technique [23]. Maleic anhydride grafted reclaim rubber was dissolved in toluene at room temperature for 24 h and then heated to 60 °C for 2 h. Subsequently, the obtained solution was filtered and then the filtrate was precipitated by acetone. The sample was collected and then washed several times with acetone and dried in a vacuum oven at 40 °C for 24 h. ATR-FTIR was operated with a diamond lens Attenuated Total Reflection (ATR) accessory. The spectra were obtained from 32 scans at a resolution of 4 cm^{-1} in the wave number range 4000 - 400 cm^{-1}.

The crosslink density of rubber vulcanizates

The equilibrium swelling behavior was carried out according to ASTM D471 using toluene as solvent. The vulcanizated rubber samples with a size of 10×10 mm^2 were immersed in toluene at room temperature. Crosslink density of rubber vulcanizates was determined from the swollen sample at equilibrium swelling in toluene at room temperature for 7 days. The swollen samples were weighed after blotting with tissue paper to remove the excess solvent on the sample surface. Then, the samples were dried at 60 °C in an oven until attains a constant weight. The crosslink density of rubber vulcanizates was calculated by the Flory-Rehner equation [24];

$$X_C = \frac{-[\ln(1-\upsilon_2)+\upsilon_2+\chi\upsilon_2^2]}{V_1\left(\upsilon_2^{1/3}-\frac{\upsilon_2}{2}\right)}$$

where X_C is the crosslink density (mol/cm^3), $\upsilon_2$is the rubber volume fraction in the swollen network, $V_1$is the molar volume of toluene, and χ refers to the Flory-Huggins interaction parameter between toluene and rubber ($\chi = 0.4$) [25]. The rubber volume fraction in the swollen network (υ_2) was determined by [26];

$$\upsilon_2 = \frac{m_2/\rho_2}{(m_2/\rho_2)+(m_1/\rho_1)}$$

where m_2 and m_1 are the absorbed solvent and swollen sample weights at equilibrium swelling, respectively, and $\rho_1$is the density of toluene while ρ_2 is the density of unswollen rubber vulcanizate.

Mechanical properties

Tensile properties were determined using a universal testing machine (Hounsfield Tensometer, model H 10KS, Hounsfield Test Equipment Co., Ltd, Surrey, U.K.) according to ASTM D412. The samples were tested at room temperature, with an extension speed of 500 mm/min. The hardness of rubber vulcanizates was also determined at room temperature by using a durometer Shore A (Frank GmbH, Hamburg, Germany) according to ASTM D2240.

Thermal mechanical behavior

Thermal-mechanical behavior of vulcanizated rubber samples was characterized by a temperature scanning stress relaxation (TSSR), using a TSSR instrument (Brabender GmbH, Duisburg, Germany). The TSSR method is based on a stress-relaxation test. A dumbbell-shaped specimen was used according to ISO527 (die type 5A). The sample was then placed in the test chamber and stretched to a constant tensile strain of 50 %. The resulting sample was pre-conditioned for 2 h at 23 °C. Then the sample was heated linearly with a constant heating rate of 2 °C/min from 23 to 220 °C until the stress relaxation was fully completed, or the sample ruptured.

Wettability and adhesion

The wettability at the rubber surface was examined using an optical contact angle analyzer (Data Physics, OCA25, Germany). Rubber vulcanizates were tested under ambient conditions by using deionized water as the polar liquid. The contact angles between the water and rubber surface were measured on at least 3 liquid drops.

Lab shear strength was measured to investigate the adhesion between rubber adhesive and wood surface. Wood rectangle board panels were cut into 25×100×3 mm^3 and sanded with sandpaper. The rubber adhesives were prepared by cutting the rubber compound into a small pieces and dissolving it in toluene to

make a 20 % solution. The adhesive solutions were applied onto the wood surfaces with a lap joint for a 25×25 mm^2 area of overlap. A load of about 1 kg was placed over the joint and kept for 24 h. Then, the wood joints were dried at 50 °C for 7 days to vulcanize the rubber adhesive. These wood joints were tested for lap shear strength using a universal testing machine (Hounsfield Tensometer, model H 10KS, Hounsfield Test Equipment Co., Ltd, Surrey, U.K.) according to ASTM D906.

Results and discussion

ATR-FTIR has been used to confirm the grafting reaction between RR and MA. The unreacted MA has to be eliminated because its characteristic peak may appear in the same region corresponding to RR-g-MA. Therefore, the elimination of unreacted MA is done by re-precipitation technique, as described in the previous section. The ATR-FTIR spectra of RR and RR-g-MA are shown in **Figure 1**. It is seen that the spectra of all samples showed the main characteristic peaks at the wavenumbers 2922 cm^{-1} (CH_2 asymmetry stretching), 2849 cm^{-1} (CH_2 asymmetry stretching), 1448 cm^{-1} (CH_2 bending), 1374 cm^{-1} (C–H asymmetric bending), 1010 cm^{-1} (CH_2=CH– bending) and 835 cm^{-1} (C=C bending).These absorption peaks are the characteristic peaks of rubber components [23,27-29]. In particular, the absorption peak at the wavenumber of 835 cm^{-1} corresponds to polyisoprene or natural rubbers [28,29], and the absorption peak at the wavenumber of 1010 cm^{-1} is characteristic of polybutadiene rubber [27,30]. Additionally, the maleic anhydride grafted reclaim rubber showed a new absorption peak (red line) at 1711 cm^{-1} (–C=O stretch, carbonyl group), which is attributed to the presence of MA molecules in the RR-g-MA. It confirms the grafting of MA onto RR molecules.

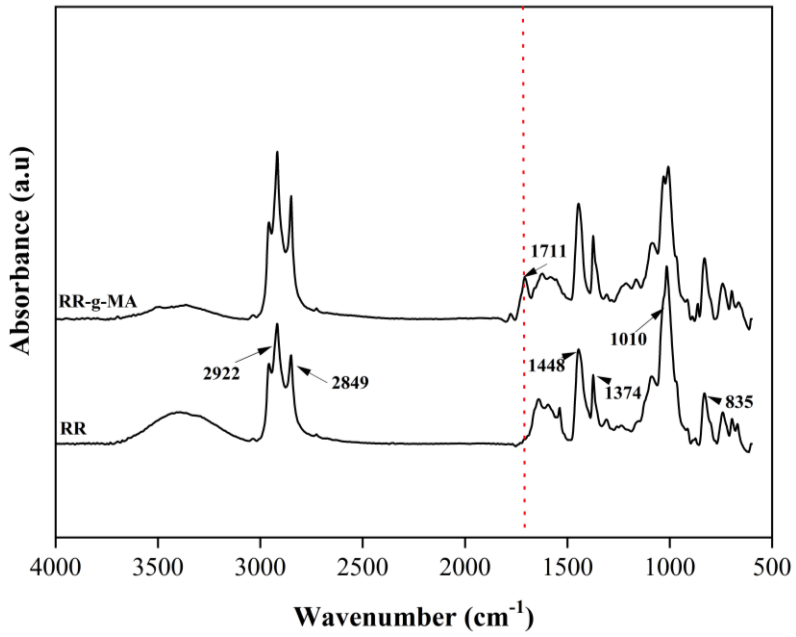

Figure 1 ATR-FTIR spectra of RR and RR-g-MA.

The crosslink density of pure ENR, ENR with RR, and RR-g-MA are calculated, and the results are shown in **Figure 2**. It can be seen that the crosslink density of ENR is increased upon the addition of RR. The incorporation of RR affects the crosslink density of rubber vulcanizates due to the presence of residual active cross-linking sites in the RR which continuously forms crosslinking during the process of vulcanization [31,32]. Moreover, ENR/RR-g-MA blends show higher crosslink density than that ENR/RR blends. This is due to the crosslinking of ENR in the ENR/RR-g-MA blends not only from the sulfidic linkage of the sulfur vulcanizates system but also from the formation of ester linkages from the reaction between the epoxide ring of ENR and MA from RR-g-MA. It has been reported that ENR can be thermally crosslinked in the presence of MA without any additional catalyst, and the degree of crosslinking depends on the MA content [33].

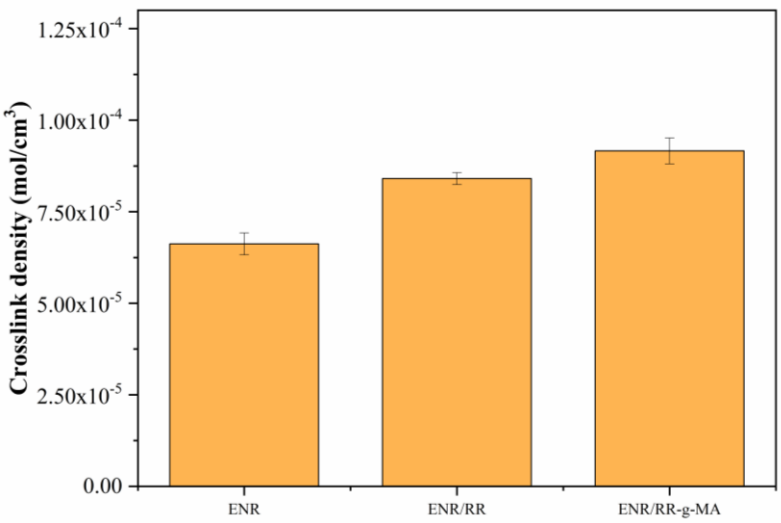

Figure 2 Crosslink density of ENR, ENR/RR, and ENR/RR-g-MA blends vulcanizates.

To verify the formation of ester linkages between the ENR chains by MA, the ATR-FTIR is used to reveal the newly generated ester linkage as shown in **Figure 3**. It is found that the ATR-FTIR spectra of ENR/RR and ENR/RR-g-MA exhibit all the characteristic peaks of RR at the wavenumbers of 2922, 2849, 1448, 1374, 1010 and 835 cm^{-1}, as mentioned in **Figure 1** result. Additionally, the absorption peaks at the wave numbers 1248 cm^{-1} and 870 cm^{-1} are assigned to the –C–H stretching of saturated chain in ENR and epoxy groups in ENR molecules, respectively. Besides, the blend of ENR/RR-g-MA showed a new absorption peak at the wavenumber of 1735 cm^{-1} which corresponds to C=O stretching of ester functionality [33,34]. This indicated the presence of ester linkage in the ENR blends with RR-g-MA. The scheme of possible crosslink formation is shown in **Figure 4**. It is found that ENR chains formed the sulfidic linkages between rubber molecules. Addition of RR results in more dense sulfidic linkage as previously discussed. Furthermore, the addition of RR-g-MA caused to generation of new ester linkage between ENR rubber chains.

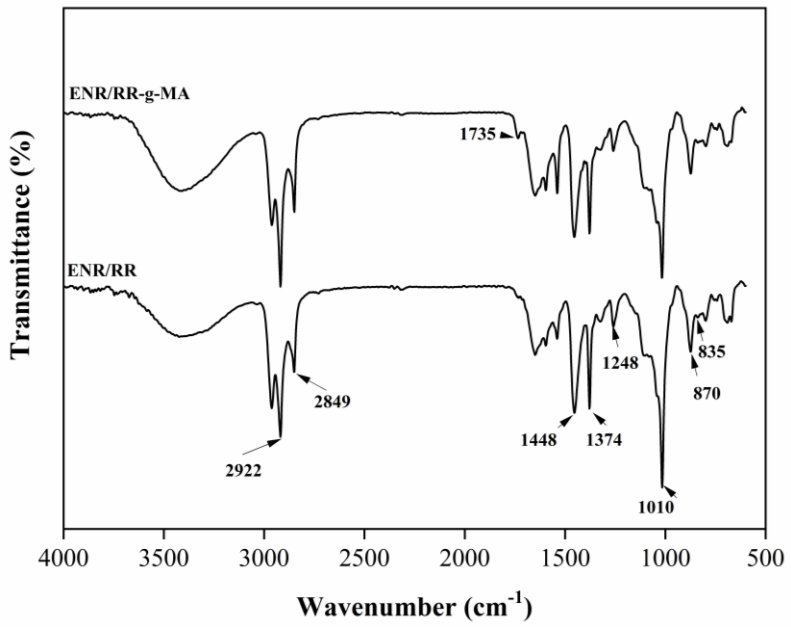

Figure 3 ATR-FTIR spectra of ENR/RR and ENR/RR-g-MA blends vulcanizates.

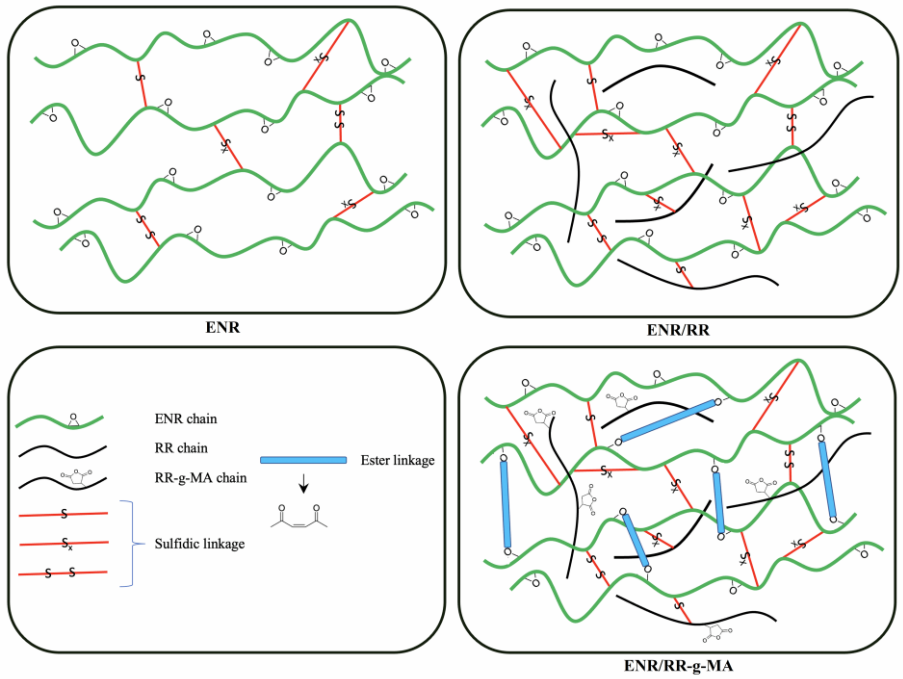

Figure 4 The scheme of possible crosslink formation of ENR, ENR/RR and ENR/RR-g-MA vulcanizates.

The mechanical properties in terms of tensile strength, elongation at break, modulus at 100 % and 300 % elongations, and hardness are summarized in **Table 2**. It is apparent that tensile strength decreased with the addition of RR and RR-g-MA. This is due to the low molecular weight of RR which would result in deterioration in the physical properties of rubber vulcanizates. During the reclamation process, severely high shear and high temperature are used to break down the rubber chains into shorter segments and lower their molecular weight. Then, the addition of lower molecular weight portion results in a progressive reduction in the tensile strength [35]. In addition, the samples exhibit a similar trend in cases of modulus at 100 and 300 % elongations and hardness. ENR exhibited the lowest values, followed by ENR/RR and ENR/RR-g-MA, respectively. While the elongation at break of rubber vulcanizate showed the opposite trend. This might be explained in terms of the reinforcing filler effect of carbon black in RR together with the crosslinking facilitated by it, which restricts the molecular mobility under tension force, and hence increased their modulus and hardness, and decreased the elongation at break of the rubber vulcanizate.

Table 2 Mechanical properties of ENR, ENR/RR blends, and ENR/RR-g-MA blends.

Samples	Tensile strength (MPa)	Elongation at break (%)	Modulus at 100 % (MPa)	Modulus at 300 % (MPa)	Hardness (shore A)
ENR	13.6±0.5	685±32	0.66±0.80	1.08±0.07	38.1±.2.9
ENR/RR	8.9±0.7	460±7	0.70±0.12	2.44±0.10	46.7±2.3
ENR/RR-g-MA	7.1±0.6	247±28	0.90±0.07	2.98±0.09	48.8±0.7

Figure 5 shows normalized force-temperature curves of ENR, ENR/RR blends, and ENR/RR-g-MA blends. Normalized force is defined as the force ratio $F(T)/F_0$, where F(T) is the force at temperature T and F_0 is the force at starting temperature. From normalized force-temperature curves, T_{10}, T_{50}, and T_{90} are calculated. It is noted that T_x indicates the temperature at which the normalized force has decreased x %. The temperatures T_{10}, T_{50}, and T_{90} are commonly identified with the thermal stability of rubber vulcanizates. A decrease in normalized force can be seen in the temperature range from 100 to 220 °C. This is attributed to the thermo-oxidative chain scission of rubber molecules, together with the breakdown of the crosslink network in the rubber vulcanizates [36]. From **Figure 5**, the thermal stability of ENR is found to be enhanced by the addition of RR and RR-g-MA. Additionally, the ENR vulcanizates with RR-g-MA

exhibited superior thermal stability when compared to those with RR. This is attributed to the higher level of crosslink density together with better thermal stability arising from ester linkage.

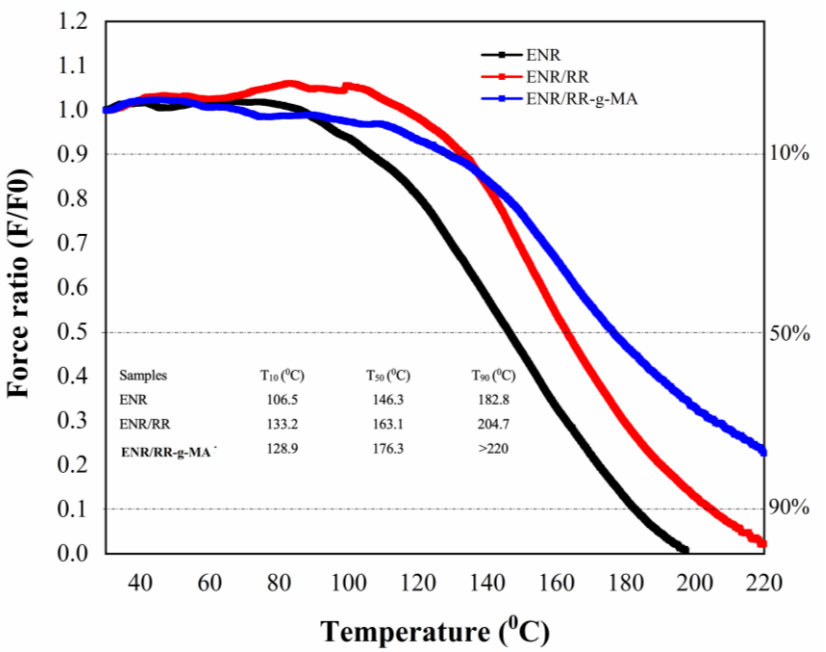

Figure 5 Normalized force-temperature curves of ENR, ENR/RR blends and ENR/RR-g-MA blends.

Contact angle gives information related to the polarity of rubber and the wettability of the surface. **Figure 6** shows the contact angles of ENR, ENR/RR blends and ENR/RR-g-MA blends. It is seen that the addition of RR does not significantly affect the contact angle of rubber blends, while the contact angle is decreased upon the addition of RR-g-MA. It is noted that a decrease in contact angle indicates an increased polarity and also wettability of the surface [37]. This result is directly related to the maleic group present in RR-g-MA, which increases the polarity and wettability of rubber blends. But, in the case of the reclaimed rubber, there is no change in the contact angle as a result of the unaffected polarity of rubber blends.

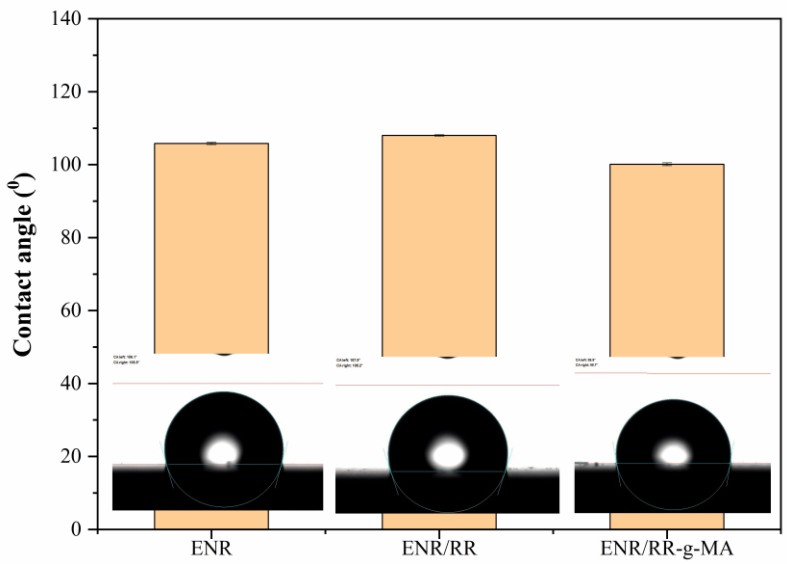

Figure 6 Contact angle of ENR, ENR/RR blends and ENR/RR-g-MA blends.

Lap shear strength of ENR, ENR/RR blend, and ENR/RR-g-MA blends are shown in **Figure 7**. The results show that the addition of both RR and RR-g-MA improved the lap shear strength of rubber adhesive. This might be attributed to the greater crosslink density that gives rise to the enhancement of the cohesive strength of rubber adhesive. Moreover, it is found that the lap shear strength of ENR/RR-g-MA blend exhibited a higher value than that of the ENR/RR blend. This is attributed to the synergistic effect of polarity and wettability of RR-g-MA towards enhanced interfacial adhesion and compatibility with the wood surfaces. Consequently, greater lap shear is observed.

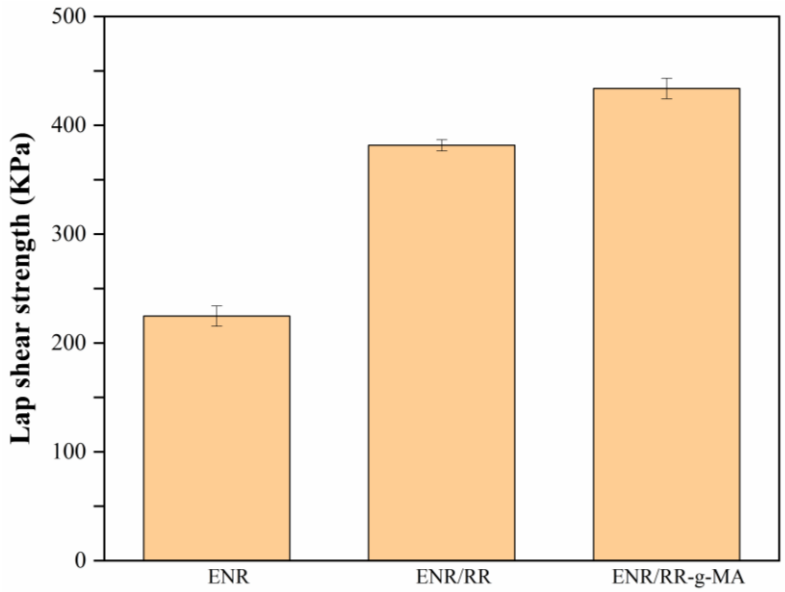

Figure 7 Lap shear strength of ENR, ENR/RR blends and ENR/RR-g-MA blend adhesives.

The adhesive fracture and the scheme of possible interaction between rubber and wood surfaces are shown in **Figure 8**. For ENR and ENR/RR adhesives, the possible interaction between rubber adhesives and wood might be generated from the hydroxy group in cellulose and the oxirane rings of ENR (red color). In the case of ENR/RR-g-MA adhesive, it has an additional interaction between the hydroxy group in cellulose and the maleic group of RR-g-MA (green color), or the ester group of ester linkage (blue color). The fracture of surfaces fixed with ENR/RR adhesive showed a type of adhesive fracture where one of the wood surfaces is covered with the adhesive. Whereas the wood samples were fixed with ENR/RR-g-MA adhesive, the fractured surfaces were exhibited in such a way that both wood surfaces are covered with adhesive and it reveals the cohesive fracture type. The improved adhesive strength in the case of wood samples joined with ENR/RR-g-MA adhesive is affected by the higher interaction between adhesive and wood surface.

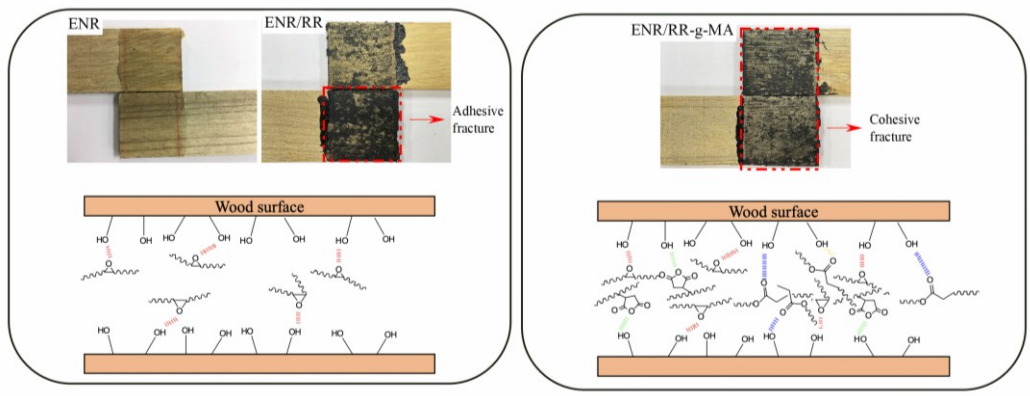

Figure 8 Adhesive fracture and the scheme of possible interaction between rubber adhesives and wood surfaces.

Conclusions

RR was successfully grafted by MA to develop effective adhesives. The influence of RR and RR-g-MA on the adhesion of ENR adhesive and related properties was studied. The addition of RR and RR-g-MA increased the crosslink density of rubber blends, especially in the case of RR-g-MA. This is due to the formation of a new ester crosslinking network by the addition of RR-g-MA which increased crosslink density. Additionally, the incorporation of RR-g-MA showed superior thermal stability due to its higher crosslink density and synergism from ester linkage. On the aspect of wettability and adhesion, RR-g-MA improved the wettability of surface and lap shear strength of rubber adhesive. This enhancement is the consequence of increased polarity of rubber blends and high adhesion strength originating from the interaction between the hydroxyl group in cellulose on the wood surface and the polar functional group of rubber adhesive. In conclusion, the worn-out rubber tire as a mass waste can be utilized to develop effective adhesives.

Acknowledgments

The authors gratefully acknowledge the financial support from the Rajamangala University of Technology Srivijaya, Thailand.

References

[1] F Pacheco-Torgal, Y Ding and S Jalali. Properties and durability of concrete containing polymeric wastes (tyre rubber and polyethylene terephthalate bottles): An overview. *Constr. Build. Mater.* 2012; **30**, 714-24.

[2] K Formela. Waste tire rubber-based materials: Processing, performance properties and development strategies. *Adv. Ind. Eng. Polym. Res.* 2022; **5**, 234-47.

[3] MR Islam, MN Islam, NN Mustafi, MA Rahim and H Haniu. Thermal recycling of solid tire wastes for alternative liquid fuel: the first commercial step in Bangladesh. *Proc. Eng.* 2013; **56**, 573-82.

[4] X Xu, Z Leng, J Lan, W Wang, J Yu, Y Bai, A Sreeram and J Hu. Sustainable practice in pavement engineering through value-added collective recycling of waste plastic and waste tyre rubber. *Eng.* 2021; **7**, 857-67.

[5] K Korniejenko, B Kozub, A Bąk, P Balamurugan, M Uthayakumar and G Furtos. Tackling the circular economy challenges - Composites recycling: Used tyres, wind turbine blades, and solar panels. *J. Compos. Sci.* 2021; **5**, 243.

[6] S Ramarad, CT Ratnam, Y Munusamy, NA Rahim and M Muniyadi. Thermochemical compatibilization of reclaimed tire rubber/poly (ethylene-co-vinyl acetate) blend using electron beam irradiation and amine-based chemical. *J. Polym. Res*. 2021; **28**, 389.

[7] M Belhaj, P Vacková and J Valentin. Evaluation of an asphalt mixture containing a high content of reclaimed asphalt and different crumb rubber modified binders. *Slovak J. Civ. Eng.* 2021; **29**, 22-30.

[8] M Shabani and M Jamshidi. Recycling NR/SBR waste using probe sonication as a new devulcanizing method; study on influencing parameters. *RSC Adv*. 2022; **12**, 26264-76.

[9] M Molanorouzi and SO Mohaved. Reclaiming waste tire rubber by an irradiation technique. *Polym. Degrad. Stab.* 2016; **128**, 115-25.

[10] D De, PK Panda, M Roy amd S Bhunia. Reinforcing effect of reclaim rubber on natural rubber/polybutadiene rubber blends. *Mater. Des.* 2013; **46**, 142-50.

[11] JI Gumede, J Carson, SP Hlangothi and LL Bolo. Effect of single-walled carbon nanotubes on the cure and mechanical properties of reclaimed rubber/natural rubber blends. *Mater. Today Commun.* 2020; **23**, 100852.

[12] NS Saimi, SN Mamauod, NA Majid, SS Sarkawi and ZZ Abidin. Mechanical properties of tire reclaimed rubber/NR blends: effect of blend ratios. *In*: Proceedings of the 6th International Conference on Green Design and Manufacture, Arau, Malaysia. 2020, p. 020116.

[13] X Zhao, H Hu, D Zhang, Z Zhang, S Peng and Y Sun. Curing behaviors, mechanical properties, dynamic mechanical analysis and morphologies of natural rubber vulcanizates containing reclaimed rubber. *e-Polymers* 2019; **19**, 482-8.

[14] PA Nelson and SKN Kutty. Cure characteristics and mechanical properties of butadiene rubber/whole tyre reclaimed rubber blends. *Prog. Rubber Plast. Recycl. Tech.* 2002; **18**, 85-97.

[15] KF El-Nemr, HA Raslan, MA Ali, MM Hasan. Innovative γ rays irradiated styrene butadiene rubber/reclaimed waste tire rubber blends: A comparative study using mechano-chemical and microwave devulcanizing methods. *J. Polym. Eng.* 2020; **40**, 267-77.

[16] MA Ali, HA Raslan, KF El-Nemr and MM Hassan. Thermal and mechanical behavior of SBR/devulcanized waste tire rubber blends using mechano-chemical and microwave methods. *J. Polym. Eng.* 2020; **40**, 815-22.
[17] TD Sreeja and SKN Kutty. Styrene butadiene rubber/reclaimed rubber blends. *Int. J. Polym. Mater. Polym. Biomater.* 2003; **52**, 599-609.
[18] D De, A Das, D De, PK Panda, B Dey and BC Roy. Reinforcing effect of silica on the properties of styrene butadiene rubber–reclaim rubber blend system. *J. Appl. Polym. Sci*. 2006; **99**, 957-68.
[19] A Salimi, F Abbassi-Sourki, M Karrabi and MH Ghoreishy. Investigation on viscoelastic behavior of virgin EPDM/reclaimed rubber blends using Generalized Maxwell Model (GMM). *Polym. Test.* 2021; **93**, 106989.
[20] M Sabzekar, MP Chenar, G Zohuri and SM Mortazavi. Investigation of mechanical, thermal, and morphological properties of EPDM compounds containing reclaimed rubber. *Rubber Chem. Technol*. 2017; **90**, 765-76.
[21] Ł Zedler, M Przybysz, M Klein, MR Saeb and K Formela. Processing, physico-mechanical and thermal properties of reclaimed GTR and NBR/reclaimed GTR blends as function of various additives. *Polym. Degrad. Stab.* 2017; **143**, 186-95.
[22] SM Morsi, HA Mohamed and SH El-Sabbagh. Polyesteramidesulfone as novel reinforcement and antioxidant nanofiller for NBR blended with reclaimed natural rubber. *Mater. Chem. Phys*. 2019; **224**, 206-16.
[23] E Kalkornsurapranee, N Vennemann, C Kummerlöwe, C Nakason. Novel thermoplastic natural rubber based on thermoplastic polyurethane blends: Influence of modified natural rubbers on properties of the blends. *Iran. Polym. J*. 2012; **21**, 689-700.
[24] PJ Flory and JJ Rehner. Statistical mechanics of cross-linked polymer networks I. Rubberlike elasticity. *J. Chem. Phys.* 1943; **11**, 512-20.
[25] N Tangboriboon, S Chaisakrenon, A Banchong, R Kunanuruksapong and A Sirivat. Mechanical and electrical properties of alumina/natural rubber composites. *J. Elastomers Plast*. 2012; **44**, 21-41.
[26] SS Choi and E Kim. A novel system for measurement of types and densities of sulfur crosslinks of a filled rubber vulcanizate. *Polym. Test*. 2015; **42**, 62-8.
[27] VM Litvinov and PP De. *Spectroscopy of rubbers and rubbery materials*. Smithers Rapra Publishing, London, 2002.
[28] EJ Guidelli, AP Ramos, ME Zaniquelli and O Baffa. Green synthesis of colloidal silver nanoparticles using natural rubber latex extracted from Hevea brasiliensis. *Spectrochim. Acta Mol. Biomol. Spectros.* 2011; **82**, 140-5.
[29] KA Dubkov, SV Semikolenov, DP Ivanov, DE Babushkin and VD Voronchikhin. Scrap tyre rubber depolymerization by nitrous oxide: products and mechanism of reaction. *Iran. Polym. J.* 2014; **23**, 881-90.
[30] KF El-Nemr, MA Ali, MM Hassan and HE Hamed. Features of the structure and properties of radiation vulcanizates based on blends of polybutadiene and ethylene-propylene diene rubber. *J. Vinyl Add. Tech*. 2019; **25**, E64-E72.
[31] C Kumnuantip and N Sombatsompop. Dynamic mechanical properties and swelling behaviour of NR/reclaimed rubber blends. *Mater. Lett.* 2003; **57**, 3167-74.
[32] D De, PK Panda, M Roy and S Bhunia. Reinforcing effect of reclaim rubber on natural rubber/polybutadiene rubber blends. *Mater. Des.* 2013; **46**, 142-50.
[33] N Srirachya, T Kobayashi and K Boonkerd. An alternative crosslinking of epoxidized natural rubber with maleic anhydride. *Key Eng. Mater.* 2017; **748**, 84-90.
[34] B Algaily, W Kaewsakul, SS Sarkawi, E Kalkornsurapranee. Enabling reprocessability of ENR-based vulcanisates by thermochemically exchangeable ester crosslinks. *Plast. Rubber Compos.* 2021; **50**, 315-28.
[35] MM Hassan, GA Mahmoud, HH El-Nahas and ES Hegazy. Reinforced material from reclaimed rubber/natural rubber, using electron beam and thermal treatment. *J. Appl. Polym. Sci.* 2007; **104**, 2569-78.
[36] N Thongkong, S Wisunthorn, S Pichaiyut, C Nakason and S Kiatkamjornwong. Natural rubber nanocomposites based on hybrid filler of zinc nanoparticles and carbon nanotubes: Electrical conductivity and other related properties. *eXPRESS Polym. Lett*. 2020; **14**, 1137-54.
[37] OJ Guy and KAD Walker. *Graphene functionalization for biosensor applications*. *In*: SE Saddow (Ed.). Silicon carbide biotechnology. 2nd ed. Elsevier, Amsterdam, Netherlands, 2016, p. 85-141.